World Journal of Hepatology

Online Submissions: http://www.wjgnet.com/1948-5182office
wjh@wjgnet.com
doi:10.4254/wjh.v3.i7.184

World J Hepatol 2011 July 27; 3(7): 184-197
ISSN 1948-5182 (online)

ORIGINAL ARTICLE

Nonmuscle myosin Ⅱ regulates migration but not contraction in rat hepatic stellate cells

Cathy C Moore, Ashley M Lakner, Christopher M Yengo, Laura W Schrum

Cathy C Moore, Ashley M Lakner, Christopher M Yengo, Laura W Schrum, Department of Biology, University of North Carolina at Charlotte, Charlotte, NC 28223, United States
Laura W Schrum, Liver,Digestive and Metabolic Disorders Laboratory, Carolinas Medical Center, Charlotte, NC 28203, United States
Author contributions: Moore CC, Yengo CM and Schrum LW developed the experimental design; Moore CC performed the research; Moore CC, Lakner AM, Yengo CM and Schrum LW analyzed the data; Moore CC, Lakner AM and Schrum LW organized and edited the paper.
Supported by NIH Grant AA14891 (awarded to LS)
Correspondence to: Laura W Schrum, PhD, Research Group Director, Liver, Digestive and Metabolic Disorders Laboratory, Carolinas Medical Center, 1000 Blythe Blvd, Charlotte, NC 28203, United States. laura.schrum@carolinashealthcare.org
Telephone: +1-704-3559670 Fax:+1-704-3557648
Received: January 6, 2011 Revised: May 6, 2011
Accepted: May 13, 2011
Published online: July 27, 2011

Abstract

AIM: To identify and characterize the function of nonmu-scle myosin Ⅱ (NMM Ⅱ) isoforms in primary rat hepatic stellate cells (HSCs).

METHODS: Primary HSCs were isolated from male Spra-gue-Dawley rats by pronase/collagenase digestion. Total RNA and protein were harvested from quiescent and culture-activated HSCs. NMM Ⅱ isoform (Ⅱ-A, Ⅱ-B and Ⅱ-C) gene and protein expression were measured by RealTime polymerase chain reaction and Western blot analyses respectively. NMM Ⅱ protein localization was visualized *in vitro* using immunocytochemical analysis. For *in vivo* assessment, liver tissue was harvested from bile duct-ligated (BDL) rats and NMM Ⅱ isoform expression determined by immunohistochemistry. Using a selective myosin Ⅱ inhibitor and siRNA-mediated knockdown of each isoform, NMM Ⅱ functionality in primary rat HSCs was determined by contraction and migration assays.

RESULTS: NMM Ⅱ-A and Ⅱ-B mRNA expression was increased in culture-activated HSCs (Day 14) with significant increases seen in all pair-wise comparisons (Ⅱ-A: 12.67 ± 0.99 (quiescent) *vs* 17.36 ± 0.78 (Day 14), $P < 0.05$; Ⅱ-B: 4.94 ± 0.62 (quiescent) *vs* 13.90 ± 0.85 (Day 14), $P < 0.001$). Protein expression exhibited similar expression patterns (Ⅱ-A: 1.87 ± 2.50 (quiescent) *vs* 58.64 ± 8.76 (Day 14), $P < 0.05$; Ⅱ-B: 1.17 ± 1.93 (quiescent) *vs* 103.71 ± 21.73 (Day 14), $P < 0.05$). No significant differences were observed in NMM Ⅱ-C mRNA and protein expression between quiescent and activated HSCs. In culture-activated HSCs, NMM Ⅱ-A and Ⅱ-B merged with F-actin at the cellular periphery and throughout cytoplasm respectively. *In vitro* studies showed increased expression of NMM Ⅱ-B in HSCs activated by BDL compared to sham-operated animals. There were no apparent increases of NMM Ⅱ-A and Ⅱ-C protein expression in HSCs during hepatic BDL injury. To determine the contribution of NMM Ⅱ-A and Ⅱ-B to migration and contraction, NMM Ⅱ-A and Ⅱ-B expression were downregulated with siRNA. NMM Ⅱ-A and/or Ⅱ-B siRNA inhibited HSC migration by approximately 25% compared to scramble siRNA-treated cells. Conversely, siRNA-mediated NMM Ⅱ-A and Ⅱ-B inhibition had no significant effect on HSC contraction; however, contraction was inhibited with the myosin Ⅱ inhibitor, blebbistatin (38.7% ± 1.9%).

CONCLUSION: Increased expression of NMM Ⅱ-A and Ⅱ-B regulates HSC migration, while other myosin Ⅱ classes likely modulate contraction, contributing to development and severity of liver fibrosis.

Key words: Hepatic stellate cells; Nonmuscle myosin Ⅱ;

Migration; Contraction; Blebbistatin; Hepatic injury

Peer reviewers: Regina Coeli dos Santos Godenberg, PhD, Associate Professor of Physiology, Carlos Chagas Filho Biophysics Institute, Federal University of Rio de Janeiro, Av. Car-los Chagas Filho no 373, CCS, Bloco G, sala G2-053, 21941-902, Rio de Janeiro, Brazil; Can-Hua Huang, PhD, Oncopro-teomics group, The State Key Laboratory of Biotherapy, Sichuan University, No. 1 Keyuan Rd 4, Gaopeng ST, High Tech Zone, Chengdu 610041, Sichuan Province, China

Moore CC, Lakner AM, Yengo CM, Schrum LW. Nonmuscle myosin Ⅱ regulates migration but not contraction in rat hepatic stellate cells. *World J Hepatol* 2011; 3(7): 184-197 Available from: URL: http://www.wjgnet.com/1948-5182/full/v3/i7/184.htm DOI: http://dx.doi.org/10.4254/wjh.v3.i7.184

INTRODUCTION

The progressive pathology of hepatic fibrosis is characterized by continual deposition and accumulation of type I collagen heavily mediated by the hepatic stellate cell (HSC). HSCs are located in the perisinusodial space of Disse between the hepatocytes and endothelial cells and comprise approximately 15% of the normal liver[1]. These lipid rich, vitamin A storing cells produce collagen and other extracellular matrix (ECM) components for maintenance of basement membrane and regulate hepatic microcirculation by modulating sinusoidal diameter[2-4]. In diseased liver, such as steatohepatitis, fibrosis, cirrhosis or hepatocellular carcinoma, damaging stimuli trigger transdifferentiation of quiescent HSCs to an activated, wound-healing myofibroblast-like cell[5]. Activated HSCs proliferate vigorously, lose retinyl ester stores, increase expression of cytoskeletal proteins such as α smooth muscle actin and secrete numerous ECM proteins including type I collagen leading to disruption of normal liver architecture impeding liver microcirculation[5].

In addition to altering the ECM, HSC hypercontractility contributes to increased resistance of sinusoids manifesting in portal hypertension, characterized by both increased portal blood flow and intrahepatic vascular tone[6,7]. Autoregulation of microcirculation is delicately balanced by vasomodulators, such as endothelin-1 (ET-1), a potent vasoconstrictor synthesized by endothelial cells and nitric oxide, a strong vasodilator[8,9], and activated HSCs have been shown to contract in response to ET-1[10,11]. Prior to matrix and microvasculature remodeling, chemotactic factors released during injury stimulate HSC migration to damaged areas. Platelet-derived growth factor, one of the most potent chemotactic molecules, also regulates factors controlling focal adhesion formation, including myosin regulatory light chain phosphorylation[12].

Myosin proteins act as molecular motors and contribute to cellular contraction, cytokinesis and migration. Myosins bind actin filaments and generate force, using energy from ATP hydrolysis. Specifically, class Ⅱ myosins are associated with generation of contractile forces[13]. In nonmuscle cells, three isoforms of nonmuscle myosin Ⅱ (NMM Ⅱ-A, Ⅱ-B and Ⅱ-C) encoded by different genes have been identified and are expressed in multiple tissues[14-16]. Distinct enzymatic properties of each isoform confer specific functions and are important in modulating kinetic properties of the cell[17].

HSC contraction and migration are necessary for the wound-healing process and influence both development and severity of hepatic fibrosis. Recent studies examined the expression and functionality of NMM Ⅱ proteins in mouse HSCs[18,19]. Inhibition of myosin Ⅱ ATPase by blebbistatin, a cell-permeable pharmacological agent, altered HSC morphology and reduced characteristic HSC contraction; however, NMM Ⅱ isoform specificity of blebbistatin is not well understood[20]. While studies have shown the pharmacological inhibitor blocks skeletal muscle and NMM Ⅱ activity with minimal effects on smooth muscle myosin Ⅱ, others have shown that blebbistatin is specific to smooth muscle myosin Ⅱ[20-23]. Lack of specificity associated with blebbistatin requires further investigation into the distinct roles of NMM Ⅱ isoforms in the HSC. Furthermore, expression of NMM Ⅱ isoforms in HSCs *in vivo* has not been investigated. In the present study we examined expression and functionality of NMM Ⅱ isoforms in rat HSCs.

MATERIALS AND METHODS

Materials

Reagents were purchased from Sigma Aldrich (St. Louis, MO) unless otherwise indicated. ET-1 was purchased from American Peptide (Sunnyvale, CA). TRIzol, Lipofecatmine and Superscript Ⅱ kit were purchased from Invitrogen Corporation (Baltimore, MD). Blebbistatin was purchased from Calbiochem (San Diego, CA). Type Ⅰ collagen was purchased from BD Biosciences (Franklin Lakes, NJ). Pronase and SYBR Green were purchased from Roche Molecular Biochemicals (Chicago, IL). Oligonucleotide primers were designed using Primer3 (v0.4.0) and synthesized by Integrated DNA Technologies (Coralville, IA). Monoclonal antibodies specific against NMM Ⅱ-A and Ⅱ-B isoforms, GAPDH, and anti-rabbit (or goat)-HRP secondary antibodies were obtained from Santa Cruz Biotechnology, Inc (Santa Cruz, CA). NMM Ⅱ-C antibody was a gift, kindly provided by Dr. Robert Adelstein. Monoclonal antibodies specific against α smooth muscle actin (αSMA) were purchased from Dako (Glostrup, Germany). Chamber slides were purchased from Lab-Tek (Rochester, NY). Secondary fluorescent antibodies (AlexaFluro 488 anti-rabbit and 594 anti-mouse), rhodamine phalloidin and DAPI were purchased from Molecular Probes (Eugene, OR). ECL reagent was purchased from Amersham Biosciences (Piscataway, NJ). siRNAs for NMM Ⅱ isoforms (Ⅱ-A and Ⅱ-B) were purchased from Ambion (Austin, TX). Optiprep was purchased from Axis-Shield (Oslo, Norway).

Animals

Male Sprague-Dawley rats [250 g (bile duct-ligation (BDL) model); 500-650 g (primary cultures)] purchased from Charles River Laboratories (Raleigh, NC) were used in these studies. All experiments were approved by The University of North Carolina at Charlotte Institutional Animal Care and Use Committee and performed in accordance with NIH guidelines.

HSC Isolation and culture

Primary HSCs were isolated from animals following in situ liver perfusion-pronase/type I collagenase digestion[24]. The liver was perfused with calcium free-buffered saline, pronase (0.035% b.w.) and collagenase (1 mg/mL) for 10 min each. Digested liver suspension was centrifuged twice at 50 × r/min for 2 min. Nonparenchymal cells were recovered from the supernatant by centrifugation at 700 × r/min for 3 min. Density gradients were prepared in Optiprep 40% (*v*/*v*) solution. The gradient was centrifuged at 700 × r/min for 17 min at 25°C. HSCs were recovered from the interface between the medium and density layer, washed and centrifuged at 700 × r/min for 5 min. Typical cell purity following isolation was ≥ 95% as determined by autofluorescence of stored retinoid esters in HSCs. Cell viability was determined by Trypan blue exclusion staining. Cells were either used immediately (quiescent) or cultured on plastic using DMEM supplemented with 10% fetal bovine serum, L-glutamine (2 mmol/L) and antibiotics (activated) as described previously[24]. Growth medium was changed on a daily basis for the first week in culture. Culturing HSCs on plastic is routinely used to mimic the *in vivo* activation process[25].

Surgical procedures

Animals were randomized into two groups; sham and BDL and allowed to recover for two weeks.

Sham: Surgical anesthesia was induced by isoflurane inha-lation and a midline laparotomy performed and closed in two layers.

BDL: Surgical anesthesia was induced by isoflurane inhalation and a midline laparotomy performed. The hepatic bile duct was exposed, double ligated, transected and the abdominal incision closed in two layers.

Post-operative care: In all experimental groups, animals received saline [0.9% (*w*/*v*)] resuscitation and buprenorphine (0.03 mg/kg, *s.q.*) immediately after each procedure. Buprenorphine was administered for the duration of the experiment as determined by the in-house veterinarian. The time points for data analysis were chosen as mild fibrosis ensued to identify specific changes in NMM Ⅱ isoform expression in the liver.

Tissue collection: Two weeks after BDL, animals were sacrificed by exsanguination and the liver resected. Tissue samples (100-200 mg) were fixed in formalin solution overnight and paraffin-embedded.

Table 1 Intron-spanning primers for the amplification of NMM Ⅱ isoforms

Gene	Sense	Anti-sense	Product length (bp)
rMyh9	5′ aga aaa ccg cat cac cat tc	5′ tgt tct tca tca gcc act cg	189
rMyh10	5′ ggc act gga gga act ctc tg	5′ ctt ctt cca gca ggg ttg ag	287
rMyh14	5′ gct gct caa gga cca tta cc	5′ gta cca gct tgc cag aga gg	275

Gene name: rMyh9: Rat nonmuscle myosin Ⅱ-A; rMyh10: Rat nonmuscle myosin Ⅱ-B, rMyh14: Rat nonmuscle myosin Ⅱ-C.

mRNA analysis

Total RNA from quiescent and culture-activated HSCs was isolated using TRIzol, DNase treated, reverse transcribed using Superscript Ⅱ following manufacturer's recommendations. RealTime PCR was run at 94°C 15 s; 58°C 25 s; 72°C 20 s, read 5 s using primers specific against NMM Ⅱ-A, Ⅱ-B and Ⅱ-C (Table 1). Reaction mixture consisted of 1 μL each of cDNA, forward and reverse primers (5 nmol), 2 μL DEPC water, and 5 μL of SYBR Green Master Mix. cDNA concentration was used as a reference to normalize samples since the expression of housekeeping genes was modulated through days in culture[24]. Data were reported as cross-point, the point at which the detectable level of SYBR green fluorescence was detected above the background. All experiments were performed a minimum of three times.

Protein analysis

Western blot: Protein expression of NMM Ⅱ isoforms during transdifferentiation of quiescent (freshly isolated), Day 1 (early activation) and Day 14 (late activation) HSCs was determined by an actin-selection assay[26]. Briefly, HSCs were homogenized in lysis buffer (50 mmol/L Tris-HCl, 0.1 mmol/L EDTA, 1 mmol/L phenylmethylsulfonyl fluoride, 2% (*w*/*v*) SDS, aprotinin and protease inhibitor cocktail). Sample lysates were equalized for protein concentration using the Bradford method and incubated with F-actin (10 mmol/L) for 30 min at 4°C. The protein complex was centrifuged at 320 000 × r/min for 30 min and the pellet suspended in Laemmli buffer. Immunoblot analysis was performed using 8% SDS-PAGE. Primary antibodies were diluted 1:500 (NMM Ⅱ-A, Ⅱ-B, or Ⅱ-C) and incubated at 4°C overnight. Secondary antibody (anti-rabbit-HRP) was used at a dilution of 1:1000 and incubated for 1 h at room temperature. Rat-1 cell line was used as a positive control for NMM Ⅱ isoform detection. Protein expression of NMM Ⅱ-A and Ⅱ-B siRNA inhibition was determined by standard Western blot analysis[27]. Briefly, HSCs were homogenized in lysis buffer, equalized for protein concentration using the Bradford method and immunoblot analysis performed using 8% SDS-PAGE.

Primary antibodies were diluted 1:500 (NMM Ⅱ-A or Ⅱ-B) or 1:1000 (GAPDH) and incubated at 4°C overnight. Secondary antibody (anti-rabbit-HRP or anti-goat-HRP) was used at a dilution of 1:1000-1:5000 and incubated for 1 h at room temperature. Signal intensity was analyzed using a digital camera and densitometric analysis program (Quantity One, Bio-Rad Laboratories, Inc).

Dual fluorescent immunostaining: The expression of NMM Ⅱ isoforms was evaluated by: (1) immunocytochemistry (ICC) of culture-activated HSCs (Day 14) incubated on chamber slides and (2) immunohistochemistry (IHC) of paraffin-embedded liver sections from normal and injured liver. For immunocytochemistry, slides were washed with PBS, blocked with 5% (v/v) normal goat serum, incubated overnight at 4°C using rabbit polyclonal NMM Ⅱ-A, Ⅱ-B and Ⅱ-C antibody (1:100). Samples were washed with PBS, incubated with secondary antibody (AlexaFluro 488: 1:500) for 1 h, followed by rhodamine phalloidin in-cubation for 15 min and finally with 4, 6-diamidino-2-phenylindole, dihydrochloride (DAPI) for 5 min. For immunohistochemistry, sections were de-paraffinized and hydrated in graded ethanol. Cross-linked proteins were exposed using heat-induced epitope retrieval and proteolytic enzyme digestion. Slides were washed, blocked [0.2% (v/v) NGS] and incubated overnight at 4°C using rabbit polyclonal NMM Ⅱ-A, Ⅱ-B and Ⅱ-C antibody (1:500). In addition, mouse αSMA was used to detect activated HSCs. Slides were washed, incubated with fluorescent secondary antibodies (AlexaFluro 488 and AlexaFluro 594: 1:1000) and developed with DAPI. To demonstrate specificity immunoreactions, negative controls (normal serum from the same species replaced the primary antibody) were included for all immunoreactions. Rat-1 cell line (ICC) and lung tissue (IHC) served as positive controls for NMM Ⅱ isoform detection (data not shown). For microscopic images, cells were visualized using the Olympus IX71 microscope (Olympus America, Inc). Images of NMM Ⅱ isoforms, αSMA, F-actin and DAPI were taken separately at identical exposures and color channels merged using IMAGE-PRO software (Media Cybernetics Inc).

siRNA-mediated inhibition

Freshly isolated HSCs were seeded at 2×10^6 cells on p60 tissue culture dishes and transfected on Day 3 of culture-activation with siRNAs for NMM Ⅱ isoforms (Ⅱ-A and Ⅱ-B) using Lipofectamine reagent. In a 5 mL polystyrene tube, NMM Ⅱ isoform or scramble siRNAs (final concentration was 100 nmol/L) was incubated with 600 μL OptiMEM and vortexed. In a separate 5 mL tube, 20 μL Lipofectamine reagent was incubated with 600 μL OptiMEM and vortexed. Solutions were combined, vortexed and incubated for 30 min at room temperature. Cells were washed and incubated with 1.5 mL OptiMEM. Cells were subsequently incubated with siRNA mixtures for 8 h. At the end of the transfection period, fresh media (2.5 mL) was added to wells and incubated for 48 h prior to analysis of mRNA and protein expression, contraction and migration analyses.

Preparation of collagen lattices

Contraction of HSCs was performed in a 24-well tissue culture dish coated with collagen as described with minor modifications[8,9]. Hydrated collagen lattices were prepared using an 8:1:1 of type I collagen: 0.2 mol/L HEPES: 10 × DMEM for final collagen concentration of 3.65 mg/mL. The mixture (300 μL) was aliquoted onto each well of a 24-well plate and allowed to congeal overnight at 37°C. Cells were serum-starved 24 h prior to seeding onto the congealed collagen lattice (3×10^5 cells/well).

Contraction assay

Collagen lattices were prepared and culture-activated HSCs (Day 4) trypsinized and seeded onto the congealed collagen lattice and allowed to recover overnight. Collagen lattices were dislodged from wells with a 10 μL pipette tip. Cells were treated with ET-1(1 nmol/L) to induce contraction. Images were captured with UVP BioSpectrum AC Imagining System at indicated time points and PTI ImageMaster software was used to measure changes in collagen diameter immediately following ET-1 treatment and 24 h later. The differences in collagen diameters were reported as percentage change in collagen lattice circumference, which is reflective of ET-1-induced contraction. Assays were repeated using transfected HSCs to assess effects of siRNA knockdown on ET-1-mediated contraction.

Migration assay

A sterile pipette tip was dragged through the cell sheet, creating a cleared zone 48 h after transfection. Images were immediately taken of the scrape in four locations per dish using the Olympus IX71 microscope. Twenty-four hours later, images were taken in the exact same locations. To assess the number of migrating cells, the PTI ImageMaster software was used to measure changes in the distance traveled into the 'damaged area' (cleared zone).

Blebbistatin treatment

Collagen-seeded HSCs (Day 5) were pre-treated with increasing doses (0-25 μmol/L; 5 μmol/L increments) of the active enantiomer (-)-blebbistatin (Blebbistatin/Bleb) or inactive enantiomer (+)-blebbistatin (Vehicle) for 30 min. The collagen lattices were dislodged from the wells and incubated with ET-1 (1 nmol/L) to induce contraction. To assess HSC contraction, the PTI ImageMaster software was used to measure changes in the collagen diameter over a 24 h incubation period.

Statistical analysis

Data are presented as mean ± SE. One-way ANOVA followed by Student-Newman-Keuls post hoc test was used to assess differences between groups at different stages of activation using Sigma Stat software. Results were considered significant for $P < 0.05$.

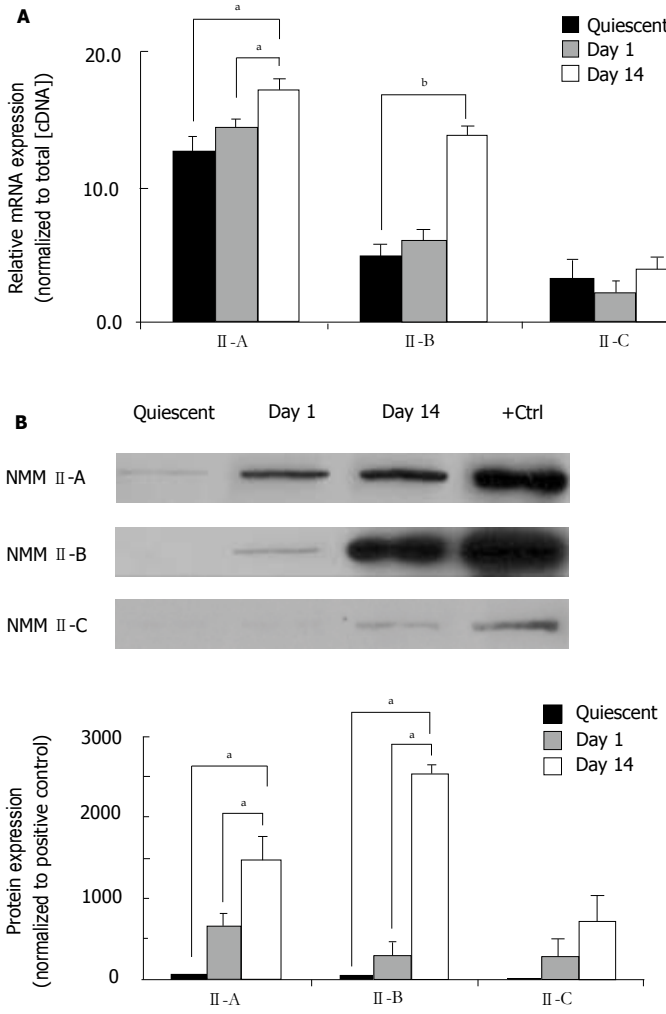

Figure 1 Relative mRNA and protein expression of nonmuscle myosin Ⅱ-A, Ⅱ-B and Ⅱ-C in hepatic stellate cells. A: mRNA expression of all isoforms was assessed in quiescent and culture-activated hepatic stellate cells (HSCs) (Day 1 and Day 14) by RealTime PCR. mRNA expression of all isoforms was normalized to total cDNA concentration. ($^aP < 0.05$; $^bP < 0.001$ as compared to quiescent). B: Protein expression of all three NMM Ⅱ isoforms was determined in quiescent and culture-activated HSCs (Day 1 and Day 14) by an actin-selection assay and subsequent Western blot analysis. Sample lysates were equalized for protein concentration using the bradford method and incubated with F-actin (10 mmol/L). (+ Ctrl; Rat-1 fibroblast cell line). Top panel: representative Western blots. Bottom panel: Western blot quantification using band intensity. ($^aP < 0.05$ as compared to quiescent).

RESULTS

NMM Ⅱ isoform expression

Throughout the HSC transdifferentiation process numerous qualitative and quantitative changes are associated with functional modifications that serve to accommodate normal or injured conditions. Our laboratory has recently demonstrated that HSC transdifferentiation from the quiescent to activated state results in significant morphological and gene expression changes[24]. Furthermore, significant alterations in the classic housekeeping genes are also present in culture activation. In the present study, we normalized gene expression in quiescent (freshly isolated), Day 1 (early activation) and Day 14 (late activation) HSCs to total cDNA concentration. RealTime PCR was performed to quantify mRNA expression of NMM Ⅱ-A and Ⅱ-B isoforms (Figure 1A). Our results demonstrate that expression was increased during transdifferentiation with significant increases seen in all pair-wise comparisons. Interestingly, mRNA expression of NMM Ⅱ-B increased 2.8-fold over culture-activation, whereas Ⅱ-A expression only increased 1.4-fold. NMM Ⅱ-C mRNA expression was not significantly altered following culture-activation. To quantify NMM Ⅱ protein we utilized an actin-selection assay, which takes advantage of the ability of actin to bind myosin in the absence of ATP[26]. Detectable levels of NMM Ⅱ-B and Ⅱ-C isoform protein expression were insignificant in quiescent HSCs (Figure 1B). Protein concentrations were doubled to verify lack of protein expression in quiescent HSCs since these results differed from mRNA expression; however, the intensities still remained negligible. Significant increases in protein expression were seen in Day 1 and Day 14 HSCs for both NMM Ⅱ-A and Ⅱ-B. NMM Ⅱ-C protein expression was also measured; however, significant levels of expression were undetected.

Cellular localization of NMM Ⅱ isoforms

Peak mRNA and protein expression levels were measured

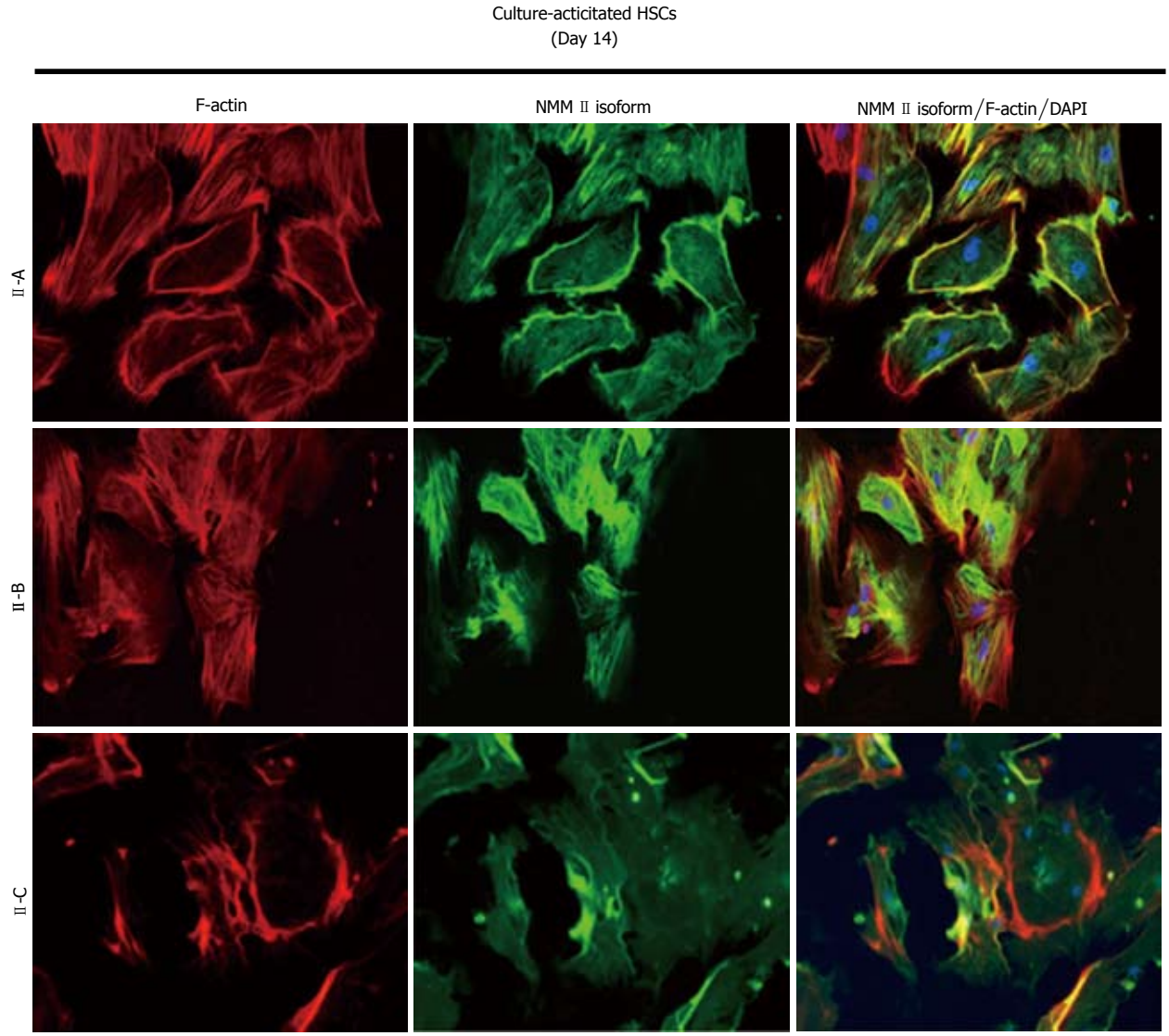

Figure 2 Immunocytochemical analysis of nonmuscle myosin Ⅱ-A, Ⅱ-B and Ⅱ-C in hepatic stellate cells. Expression of all three isoforms was detected in culture-activated cells (Day 14). Specific Ⅱ immunoreactivity of representative fields is shown in green; F-actin stress fibers (phalloidin) are shown in red and cell nuclei are stained blue (DAPI). Images of Ⅱ isoforms, F-actin, and DAPI were taken separately at identical exposures and color channels were merged using IMAGE-PRO software (350 ×).

in fully activated HSCs that are present during wound-healing; therefore, Day 14 cells were utilized for immunocytochemistry (Figure 2). Culture-activated HSCs exhibited characteristic stress fiber formation as detected by F-actin (rhodamine phalloidin) staining. All three NMM Ⅱ isoforms were detected in HSCs, which corresponded with mRNA and protein expression. Merged images revealed a stronger focus (yellow fluorescence) of NMM Ⅱ-A and Ⅱ-B with F-actin compared to Ⅱ-C. Additionally, NMM Ⅱ-A localization with F-actin showed a stronger intensity at the cell periphery, while Ⅱ-B was predominantly located throughout the cytoplasm.

NMM Ⅱ isoform expression in normal vs fibrotic liver

Increased isoform expression was seen in activated HSCs, the main effector cells in hepatic fibrosis. To confirm this observation *in vivo*, a BDL model of liver injury was utilized. BDL-induced fibrosis typically generates lesions surrounding bile duct epithelium and stimulates cholangiocyte proliferation, resulting in hepatic inflammation and injury[28]. HSCs respond to BDL-induced injury and transdifferentiate into activated myofibroblast-like cells, characterized by αSMA expression. NMM Ⅱ-A and Ⅱ-B protein expression was minimally detected in normal liver tissue, while BDL liver tissue showed up-regulation of all three NMM Ⅱ isoforms (green fluorescence), correlating with *in vitro* data. αSMA (red fluorescence) expression was observed in BDL-injured tissue (Figure 3) and, interestingly, NMM Ⅱ-B was the only isoform found to merge (yellow fluorescence) with activated HSCs in BDL liver tissue.

Inhibition of NMM Ⅱ isoforms

siRNA-mediated inhibition was utilized to perform spe-

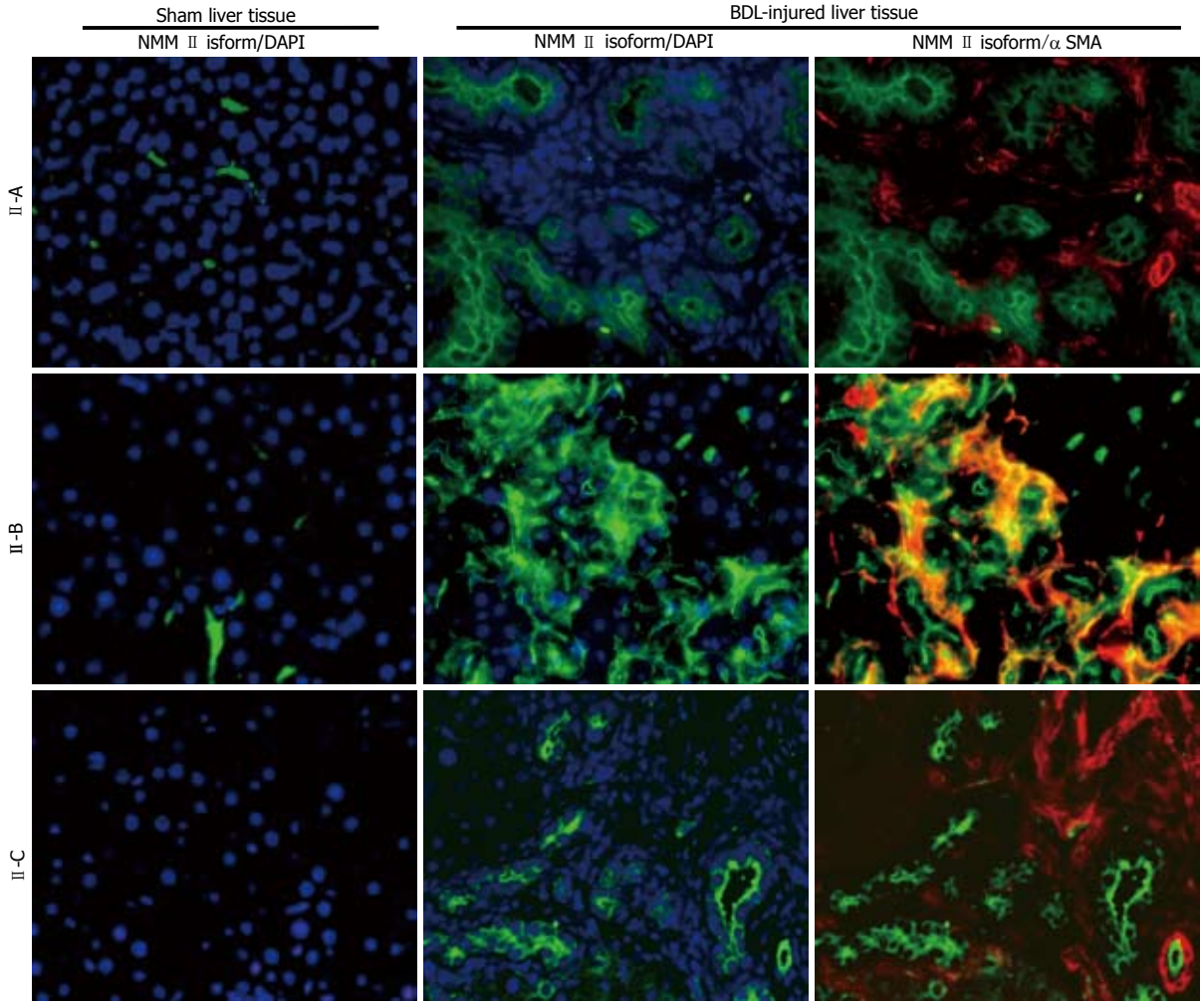

Figure 3 Immunohistochemical analysis of nonmuscle myosin Ⅱ-A, Ⅱ-B and Ⅱ-C in normal and injured liver sections. Specific nonmuscle myosin (NMM) Ⅱ immunoreactivity of representative fields is shown in green; αactin smooth muscle, as a marker of hepatic stellate cell activation is shown in red and cell nuclei are stained blue (DAPI). Images of NMM Ⅱ isoforms, F-actin, and DAPI were taken separately at identical exposures and color channels were merged using IMAGE-PRO software (200 ×).

cific knockdowns of NMM Ⅱ-A and Ⅱ-B in primary activated HSCs given that Ⅱ-C mRNA and protein expression was not significantly altered during transdifferentiation (Figure 3). Cells were transfected with the appropriate siRNA (100 nmol/L). RealTime PCR confirmed successful inhibition of NMM Ⅱ-A (60% reduction compared to scramble) (Figure 4A) and Ⅱ-B (56% reduction compared to scramble) (Figure 4B). Similarly, transfections with NMM Ⅱ-A or Ⅱ-B resulted in reduced protein expression, 52% and 49% respectively (Figure 4C and 4D). Additionally, siRNA inhibition specificity was shown as indicated by no reduction in NMM Ⅱ-A expression when transfected with Ⅱ-B siRNA alone (Figure 4A). Parallel experiments also demonstrated specific knockdown of NMM Ⅱ-B (Figure 4B).

Effect of NMM Ⅱ isoform inhibition on HSC migration and contraction

To determine functional contributions of NMM Ⅱ isoforms in the HSC, culture-activated cells (Day 5) were treated with scramble, Ⅱ-A, Ⅱ-B or Ⅱ-A and Ⅱ-B siRNAs. Using a plate scrape model of injury-induced migration, location-specific images were taken prior to and 24 h following damage and gap distance was marked and measured. As compared to the scramble siRNA, all isoform permutations displayed impaired migratory properties (Figure 5). Quantitative analysis of the change in gap distance revealed significant decreases with both siRNA treatments indicating importance of these molecular motors in HSC migration (bottom panel).

To further investigate additional known functions of NMM Ⅱ-A and Ⅱ-B, HSCs were transfected with specific siRNAs and subsequently treated with ET-1 for 24 h to induce contraction on collagen lattices. The effect of isoform inhibition was determined by changes in gel circumference after 24 h as compared to scramble control. Results indicated that siRNA-mediated knockdown did not result in inhibition of ET-1-induced contraction (Figure 6). Several adjustments to the contraction assay were made to validate results. siRNA concentration and incubation period were changed, in addition to altering matrix stiffness; however, these modifications also demonstrated

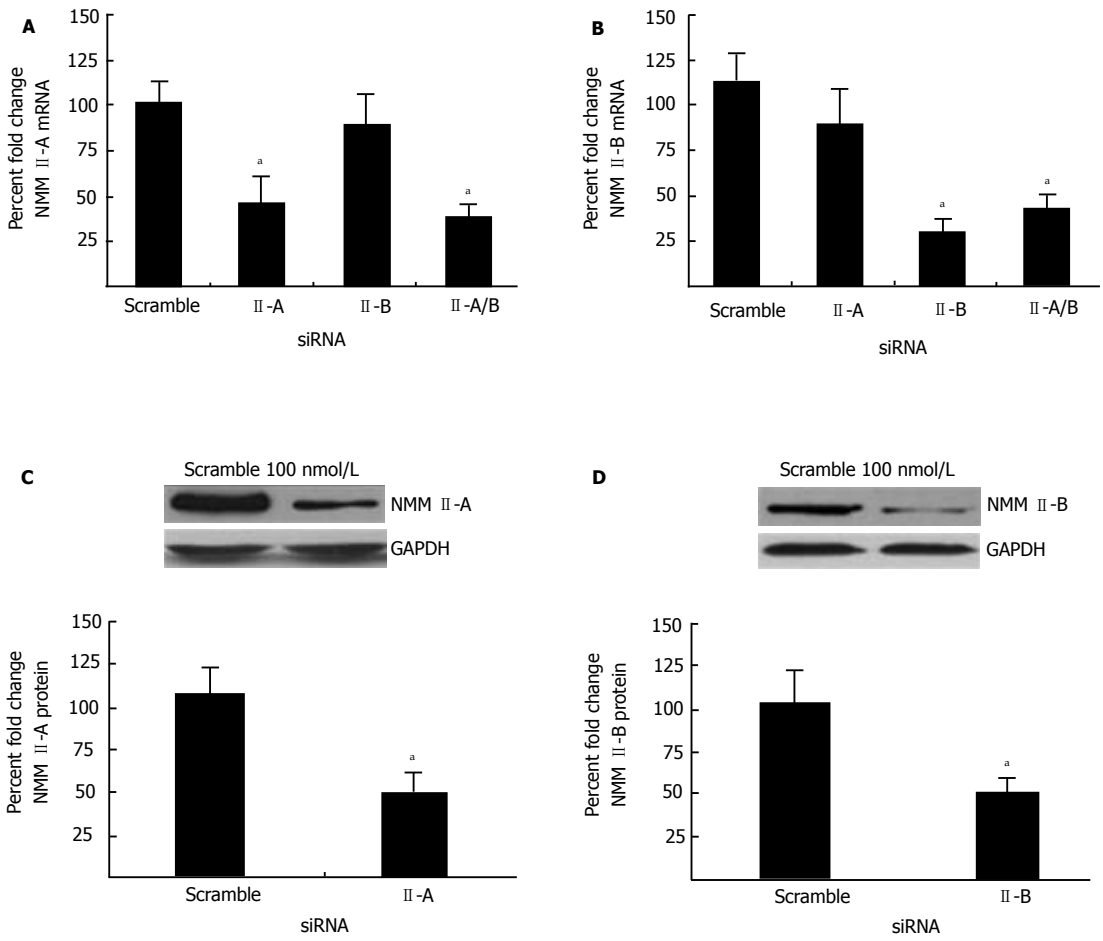

Figure 4 Nonmuscle myosin Ⅱ isoform inhibition. A and B: Culture-activated hepatic stellate cells (Day 3) were incubated with nonmuscle myosin Ⅱ-A or Ⅱ-B, Ⅱ-A & Ⅱ-B, or scramble siRNA (100 nmol/L) for 48 h. RealTime PCR determined isoform-specific inhibition of each isoform as normalized to total cDNA concentration and compared to scramble control. C and D: In parallel experiments cell lysates were isolated and protein inhibition determined by western blot analysis. Protein expression was normalized to GAPDH and compared to scramble control ($^aP < 0.05$ as compared to scramble).

that specific inhibition of NMM Ⅱ isoforms does not alter rat HSC contraction capabilities.

Chemical inhibition of NMM Ⅱ isoforms

Studies conducted utilizing culture-activated HSCs (Day 10) demonstrated myosin Ⅱ chemical inhibition significantly attenuated ET-1-induced HSC contraction[18]. However, our studies demonstrated that gene isoform inhibition by siRNA revealed no effect on contractile properties/function. Therefore, to determine possible contributions of other myosin Ⅱ family members, we used the chemical inhibitor, blebbistatin, in our studies. Day 5 HSCs are most responsive to ET-1-induced contraction[29]; therefore, Day 5 HSCs were pre-treated with increasing doses of blebbistatin (0-25 μmol/L) prior to ET-1 (1 nmol/L) treatment (Figure 7A). Twenty-four hours following chemical treatment, collagen lattice was imaged (top panel) and differences in collagen lattice diameter reported as percentage change in gel circumference (bottom panel). Consistent with previous findings, HSCs exerted a contractile force, which resulted in a 22 ± 3% decrease in collagen lattice circumference (white bar). ET-1 treatment induced hypercontraction and as expected, blebbistatin pretreatment abolished the aforementioned effect in a dose dependent manner (black bars), while vehicle pretreatment permitted ET-1-induced contraction (grey bars). Quantitative analysis revealed that 5 μmol/L blebbistatin treatment significantly reduced HSC contraction, as did higher doses of the pharmacological inhibitor. Consistent with previous findings, micrograph images of HSCs seeded onto collagen lattice exhibited a contractile star-like shape (Figure 7B). In response to ET-1 stimulus, myosin Ⅱ activation resulted in HSC elongation along the cellular axis as previous described[18,30], while chemical inhibition of myosin Ⅱ activation restored original cellular shape.

DISCUSSION

Chronic injury and unresolved fibrosis perpetuates HSC activation and further promotes the deleterious clinical effects of portal hypertension, which is associated with both increased portal blood flow and augmented intrahepatic vascular resistance[6,7]. In characterizing the expression profile of specific NMM Ⅱ isoforms during differ-

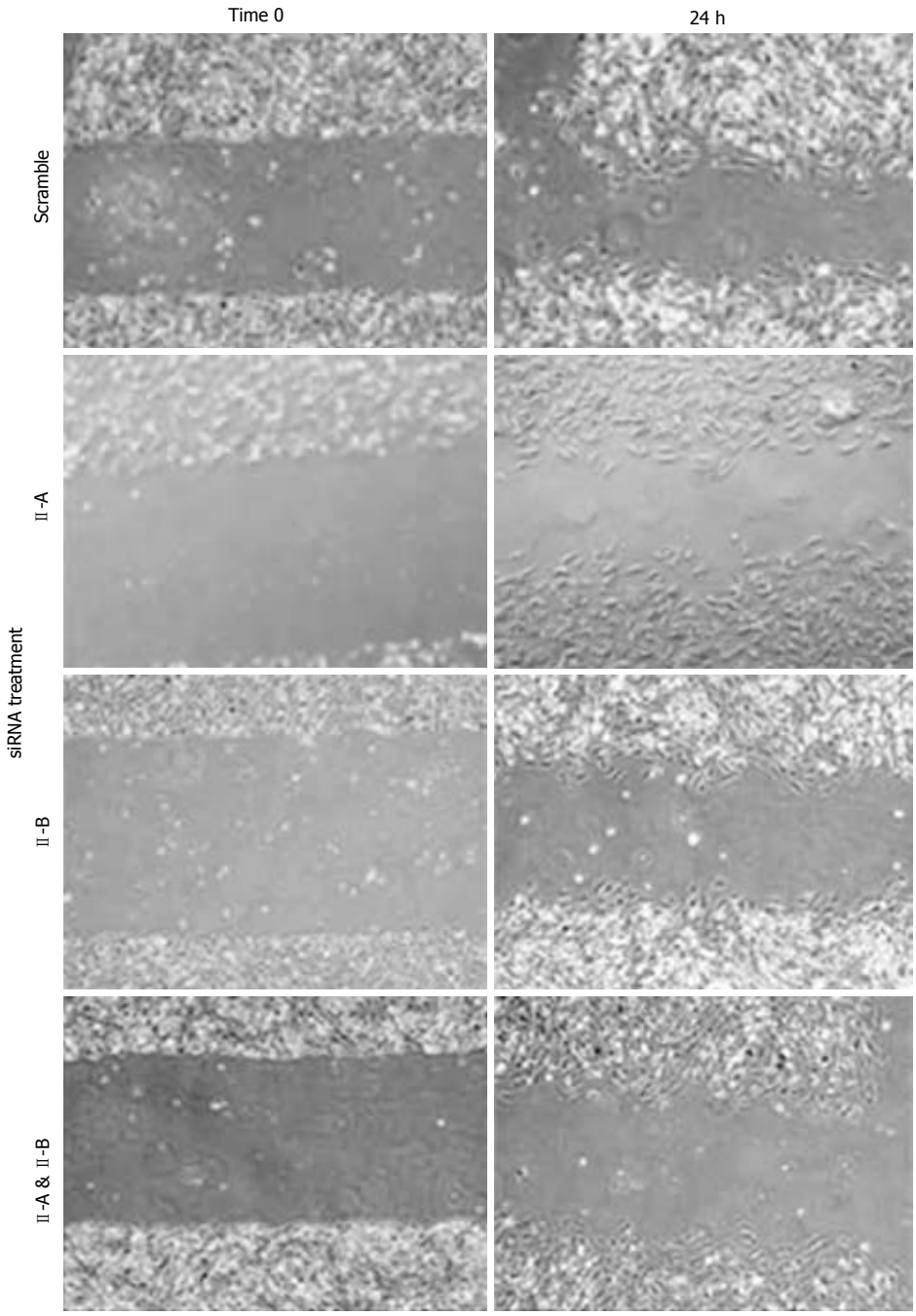

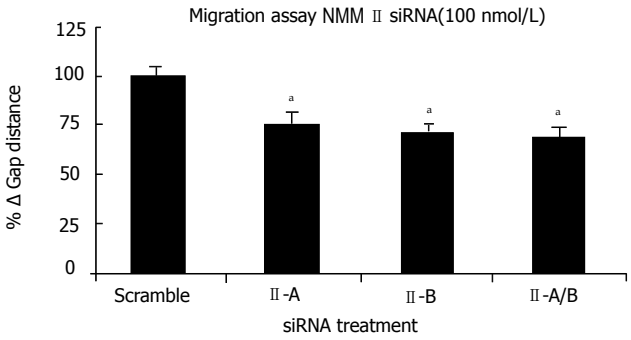

Figure 5 Effect of nonmuscle myosin Ⅱ inhibition on hepatic stellate cell migration. Culture-activated hepatic stellate cells (Day 3) were transiently transfected with siRNA targeted to all nonmuscle myosin (NMM) Ⅱ permutations (NMM Ⅱ-A, Ⅱ-B, Ⅱ-A & Ⅱ-B) or scramble siRNA and incubated for 48 h. A plate scrape model of migration was used to simulate liver injury. After 24 h, migration was calculated as change in wound (gap) diameter over time. Top panel: representative micrographs. Bottom panel: Migration assay quantification. ($^{a}P < 0.05$ as compared to scramble).

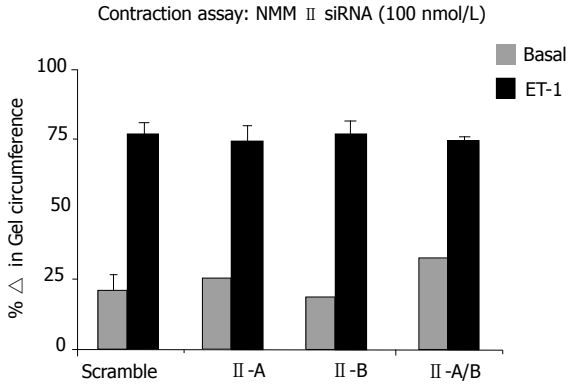

Figure 6 Effect of nonmuscle myosin Ⅱ inhibition on hepatic stellate cell contraction. Culture-activated hepatic stellate cells (Day 3) were transiently transfected with siRNA targeted to nonmuscle myosin(NMM) Ⅱ-A, Ⅱ-B, Ⅱ-A and Ⅱ-B or scramble siRNA (100 nmol/L and allowed to incubate for 24 h. Cells (1×10^5) were seeded onto collagen lattices overnight, serum-starved for 24 h and subsequently treated with ET-1 (1 nmol/L). Twenty-four hours following chemical treatment, hepatic stellate cell contraction was quantified using PTI ImageMaster software and reported as percentage change in gel circumference.

ent stages of HSC transdifferentiation, we were able to evaluate individual components that may be responsible for the fibrogenic response of activated HSC migration. In agreement with our findings, recent studies in mouse HSCs indicated that an increase in NMM Ⅱ isoform expression regulates cellular motility[18,31]; however, in contrast to these studies, we report that NMM Ⅱ isoforms in rat HSCs increases cellular migration.

Isoform-specific localization of NMM Ⅱ along actin stress fibers has previously been ascribed to cellular functions in multiple cell types[32]. Specifically, in bovine aortic endothelial cells, NMM Ⅱ-A merges with actin filaments at the leading edge of cells, while NMM Ⅱ-B merges within the cytoplasm, which facilitates endothelial cell expansion under diseases states[33]. In contrast to these findings, studies in mouse HSCs demonstrated that NMM Ⅱ-A is distributed along αSMA-containing stress fibers following culture-activation, while NMM Ⅱ-B is located at the leading edge of lamellipodia[18]. In our studies, upregulation of NMM Ⅱ-A and Ⅱ-B expression was associated with F-actin stress fibers in the cellular periphery and throughout the cytoplasm of rat HSCs respectively. These results are consistent with previous studies in fibroblast cells suggesting that NMM Ⅱ-A activation facilitates rearrangement of actin bundles into cellular protrusions and NMM Ⅱ-B incorporates into cytoplasmic stress-fibers[34].

While the expression of the NMM Ⅱ isoforms is relatively ubiquitous in most nonmuscle cells it has yet to be determined whether these proteins play redundant, overlapping or distinct roles in performing various mechanical functions in rat HSCs. Therefore, we per-formed migration and contraction studies using siRNA-mediated knockdown of NMM Ⅱ-A and Ⅱ-B, which were upregulated during culture-activation of HSCs *in vitro*. While Liu *et al* reports that siRNA-mediated NMM Ⅱ-A inhibition increased cellular migration in mouse HSCs[18,31], our studies demonstrated that NMM Ⅱ-A and Ⅱ-B knockdown significantly reduced the migratory capacity of rat HSCs. While previously studies have suggested that isoform specific rearrangement of actin stress fibers may be responsible, in part, for differences in migration rates among different cell types[32], further analysis is needed to validate these conflicting species-specific findings.

Based on the kinetic properties of NMM Ⅱ-B, it has been proposed that this isoform may be involved in maintaining tonic force needed for particular cellular functions such as hypercontraction[14]. Furthermore, it has been demonstrated that the loss of NMM Ⅱ-B decreases 3D collagen gel contraction[35]. While Liu *et al* reported that NMM Ⅱ-A is the essential isoform necessary for contraction in mouse HSCs, our results indicated that NMM Ⅱ-A and/or Ⅱ-B knockdown in rat HSCs does not significantly alter basal or ET-1-induced contraction. In order to confirm these results, we optimized our contraction assay by increasing siRNA concentration and incubation times, altering collagen lattice concentration and cell number; however, changing these parameters had no effect on HSC contraction (data not shown). In the studies performed by Meshel *et al*, NMM Ⅱ-B$^{-/-}$ fibroblast demonstrated significant differences in cell movement and contraction depending on experimental substrate[26,35]; therefore, it is possible that technical differences in experimental design may explain our conflicting results. Future studies will more closely examine the contribution of NMM Ⅱ isoforms using a Cre-lox recombination system to completely inhibit these isoforms and assess HSC hypercontraction.

While cellular localization suggests possible mechanisms by which NMM Ⅱ may function in the diseased state, further investigation *in vivo* was explored using a bile-duct ligation (BDL) model of hepatic injury. Obstruction of the common bile duct initiates rapid proliferation of biliary cholangiocytes and inflammation[36]. Following epithelial expansion, sustained blockage of bile flow causes continual activation of HSCs in the periductal region, which promotes biliary fibrosis. In our studies, NMM Ⅱ-B expression was evident in activated HSCs during BDL-induced hepatic fibrosis, while NMM Ⅱ-A and Ⅱ-C were only associated with biliary cholangiocytes. These results may suggest that NMM Ⅱ-A and Ⅱ-C may not be detectable in HSC in the *in vivo* setting. Previous studies have identified an important role for NMM Ⅱ in cellular adhesion and collagen remodeling during wound repair[26,35]. While NMM Ⅱ-B may be the important isoform contributing to the development and progression of hepatic fibrosis, NMM Ⅱ-A and Ⅱ-C may be contributing to the initiation of the inflammatory response by stabilizing integrins and other cellular adhesion molecules. Together, the *in vitro* and *in vivo* data suggest that each NMM Ⅱ isoform may be responsible for specific molecular functions during liver injury.

Although siRNA data confirmed that successful knockdown of one isoform does not influence expression of another NMM Ⅱ isoform (Figure 4A and 4B), it is plau-

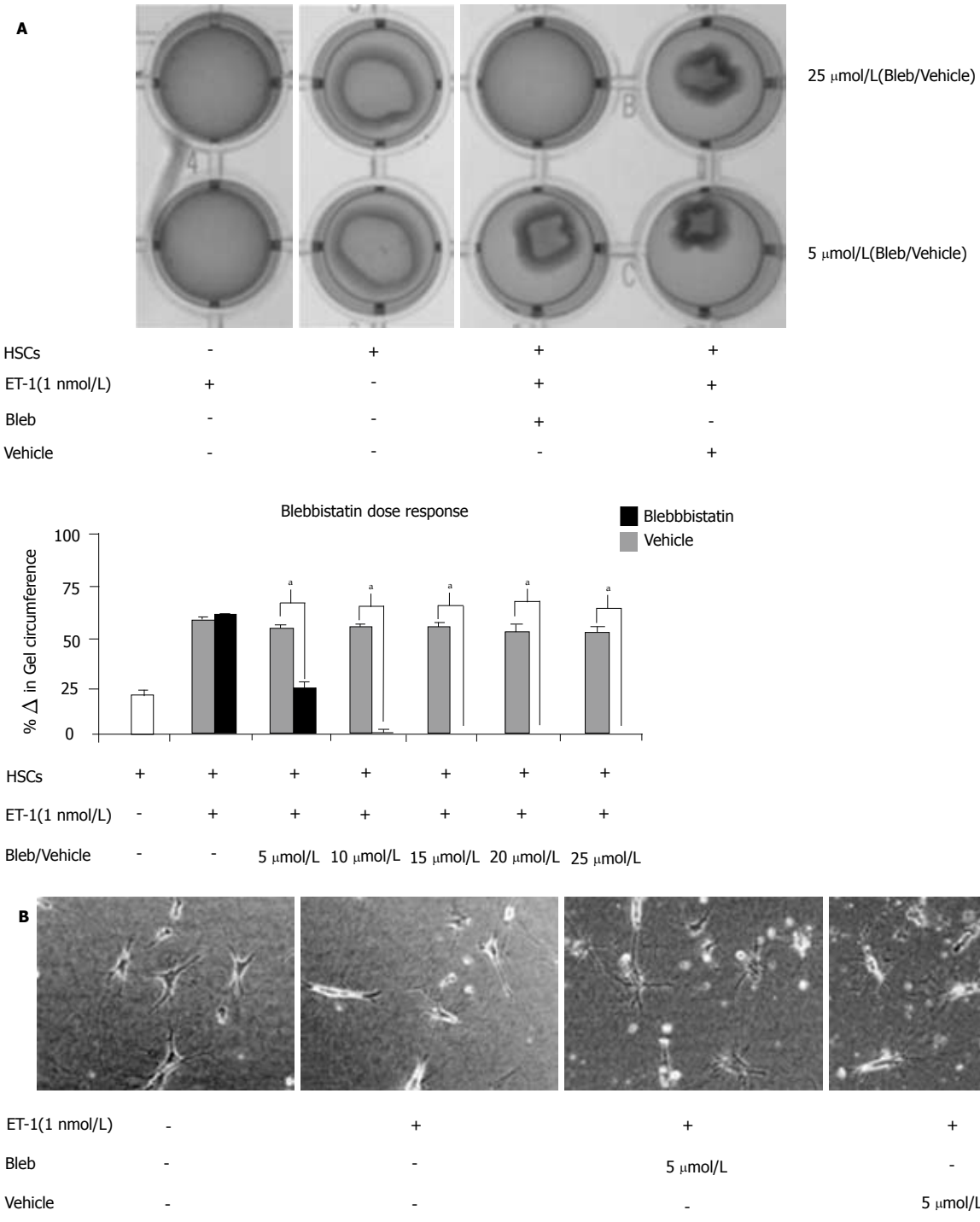

Figure 7 Blebbistatin-inhibited endothelin-1-induced hepatic stellate cell contraction. Culture-activated hepatic stellate cells(HSCs) (Day 4) were serum-starved 24 h prior to seeding onto collagen lattices (3×10^5 cells/well). Cells were pretreated with inactive (Vehicle) or active (Blebbistatin) myosin Ⅱ inhibitor in increasing doses (0-25 μmol/L; 5) and subsequently treated with blebbistatin-inhibited endothelin-1 (ET-1) (1 nmol/L) after 30 min. ($^aP < 0.05$ as compared to scramble). A: Representative light micrographs of collagen lattices: with or without seeded HSCs; with or without chemical treatments (top panel). Twenty-four hours following chemical treatment, hepatic stellate cell contraction was quantified using PTI ImageMaster software and reported as percentage change in gel circumference (bottom panel). B: Representative light micrographs of collagen-seeded HSCs with or without chemical treatments.

sible that these findings resulted from a species-specific replacement to compensate for the deficiency of one isoform by producing a functionally equivalent signaling mechanism to activate migration and contraction using other myosin Ⅱ classes. Since HSCs are nonmuscle cells, the focus of the current study was to evaluate NMM Ⅱ isoforms; however, HSCs express a large number of early and late smooth muscle cell markers including α smooth muscle (SM) actin, SM22a, desmin, SM myosin heavy chain, h1-calponin, h-caldesmon and myocardin, which also may contribute to HSC migration and hypercontraction during hepatic injury[37]. Alternatively,

HSC migration and hypercontraction may be controlled by independent signaling mechanisms that are mutually exclusive, partly explaining the observed species-specific differences. While upregulation of the Rho signaling pathway in activated HSCs confers an increase in contractile potential[38-40], Rac phosphorylation of the MHC induces filament instability, promotes disassembly of actomyosin complexes and decreases migration[41-44]. In the current studies, siRNA knockdown of NMM Ⅱ isoforms does not eliminate the possibility that actin stabilization and/or other myosin Ⅱ sub-classes may be contributing to the hypercontractile phenotype of activated HSCs. Consistent with previous reports, micrograph images from our studies suggest that ET-1-induced contraction is associated with HSC cytoskeletal remodeling and cellular hypercontraction (Figure 7B). In order to facilitate contraction, NMM Ⅱ may mediate cellular stretching and elongation, while other myosin Ⅱ classes may be responsible for coordinated force generation. Therefore, we used the chemical inhibitor blebbistatin, which has previously been shown to block protrusion-mediated lamella formation and cellular contraction[18,45]. By using this selective inhibitor, in combination with our siRNA data, we demonstrate that in rat HSCs myosin Ⅱ is the protein responsible for ET-1 induced cytoskeletal remodeling and hypercontraction; however, we concede that this controversial chemical inhibitor is not specific to NMM Ⅱ. Differences between each experimental approach suggest that other myosin Ⅱ sub-classes may also contribute to the contractile phenotype of rat HSCs.

In addition to sinusoidal constriction being associated with portal hypertension, hepatic microcirculatory failure contributes to end-organ failure in septic patients[46]. Prolonged oxygen deprivation of abdominal organs results in ischemia, tissue damage and necrosis culminating in increased mucosal permeability[47]. Endotoxin and microbial debris can subsequently penetrate the gut wall and permeate into the portal and hepatic artery where sinusoidal endothelial cells (SECs) and Kupffer cells (KCs) establish the first line of inflammatory defense[48]. KCs release a host of inflammatory cytokines, while activated SECs lose their normal anticoagulant state, promote leukocyte infiltration and increase secretion of ET-1. Neighboring HSCs are responsive to these inflammatory and vasoconstrictor signals, which promotes sustained HSC activation and contractility. Compelling evidence has demonstrated the efficacy of targeting SEC/leukocyte interactions, which improved sinusoidal congestion and portal hypertension[49]. Effective experimental treatments have also targeted KC activation, which results in preservation of hepatic function and improved survival after sepsis[50]. In addition to current treatment modalities, manipulation of migrating, hypercontractile HSCs may also improve hepatic microcirculation and patient survival during sepsis. While modulating HSC contraction may improve the microcirculation, controlling migration may prove to be beneficial in ameliorating the severity of fibrosis by decreasing the rate of collagen formation[35]. Portal hypertension remains the main cause of morbidity and mortality in patients with cirrhosis[51]. Although progress has been made in understanding the pathophysiology of portal hypertension, current pharmacological therapies have been limited to non-selective beta-blockers[52] and statins[53]; however,these treatments result in vasomodulation of the *splanchnic circulation*[54]. Given that increased hepatic microvascular resistance to portal circulation is the leading factor in cirrhotic portal hypertension, a direct molecular therapy may be more effective. Modulating intrahepatic vascular tone may provide additive benefit in patients suffering with unresolved fibrosis and cirrhosis, thus targeting all complications associated with portal hypertension. Therefore, delineating the role of NMM Ⅱ isoforms in HSC-associated portal hypertension could lead to new therapeutic targets.

ACKNOWLEDGMENTS

We would like to thank Dr. Kyle J Thompson and Whitney Ellefson for critical reading of the manuscript and Dr. Didier Dreau for his guidance with HSC migration assays (UNC-Charlotte). We appreciate the NMM Ⅱ-C antibody from Dr. Robert Adelstein (National Lung, Heart and Blood Institute). Additionally, we acknowledge guidance from Dr. Alyssa A Gulledge for assistance with primer design and RealTime PCR analysis (UNC-Charlotte).

COMMENTS

Background

Hepatic fibrosis results from normal wound-healing processes going awry and is the main cause of increased intrahepatic vascular resistance during liver injury. When the injury is chronic, type Ⅰ collagen deposition by hepatic stellate cells (HSCs) exceeds collagen resolution as a result of imbalance between fibrogenesis and fibrolysis. Altered extracellularmatrix (ECM) architecture and mechanical distortion culminates in increased blood pressure in the portal venous system, as blood must be diverted away from the liver. In addition to occlusion and compression of the microvasculature by excess collagen deposition, HSC hypercontractility contributes to increased resistance of the sinusoids leading to the clinical manifestation of portal hypertension. HSCs regulate intrahepatic vascular resistance and blood flow at the sinusoidal level through upregulation and activation of motor proteins. Specifically, HSC cytoskeletal remodeling, migration and hypercontraction has been previously associated with nonmuscle myosin (NMM) Ⅱ upregulation and activation. Function of NMM Ⅱ isoforms (Ⅱ-A, Ⅱ-B and Ⅱ-C) have been previously characterized in migrating fibroblasts and mouse HSCs, suggesting an essential role in perpetuation of chronic liver injury.

Research frontiers

Through its effects on cytoskeletal remodeling, targeting NMM Ⅱ may provide a novel mechanism to modulate multiple interrelated pathways such as cellular migration, adhesion and ECM remodeling.

Innovations and breakthroughs

Recently, Liu *et al*[18] reported that siRNA-mediated NMM Ⅱ-A inhibition increased cellular migration in mouse HSCs; however, our results suggest both NMM Ⅱ-A and Ⅱ-B mediate rat HSC migration. Consistent with findings by Vicente-Manzanares *et al*[34], our results demonstrate that NMM Ⅱ inhibition decreases cellular components associated with migration such as cytoskeletal remodeling and elongation. In addition, our studies are the first to report the expression profile of NMM Ⅱ isoforms in a fibrotic injury model *in vivo*. Finally, studies have shown the pharmacological inhibitor, blebbistatin blocks skeletal muscle and NMM Ⅱ activity with minimal effects on smooth muscle myosin Ⅱ, while others have shown that blebbistatin is specific to smooth muscle myosin Ⅱ. Conversely, we demonstrate that in rat HSCs this controversial chemical inhibitor is not specific to NMM Ⅱ.

Applications

Although progress has been made in understanding the pathophysiology of fibrosis and portal hypertension, current pharmacological therapies have been limited to treatments, which result in vasomodulation of the *splanchnic circulation*. Given that increased hepatic microvascular resistance to portal circulation is the leading factor in cirrhotic portal hypertension, a direct molecular therapy may be more effective. Modulating intrahepatic vascular tone may provide additive benefit in patients suffering with unresolved fibrosis and cirrhosis, thus targeting all complications associated with portal hypertension. Therefore, delineating the role of NMM Ⅱ isoforms in HSC-associated portal hypertension could lead to new therapeutic targets.

Terminology

Quiescent HSCs: Under physiological conditions, the inactivated cell projects extensive cytoplasmic processes through the space of Disse and reach between hepatocytes and endothelial cells wrapping around neighboring sinusoids similar to tissue pericytes suggesting a functional role in maintenance of vascular tone similar to smooth muscle cells. Quiescent HSCs also play a vital role in normal matrix maintenance and remodeling, similar to a fibroblast. Activated HSCs: HSCs proliferate, lose retinol droplets, increase expression of alpha smooth muscle actin and secrete excess type Ⅰ collagen for matrix repair. Increased micro-projections from the myofibroblast allow for increased chemotactic signaling, which induces cellular migration to the site of injury. Because of the anatomical location and increased contractile apparatus expression, it has been suggested that HSCs are capable of disrupting liver blood flow by hypercontracting, impeding microcirculation and contributing to portal hypertension. Culture-activated HSCs: Transdifferentiation of quiescent HSCs into the activated state *in vitro* is routinely accomplished by culturing cells on plastic tissue culture dishes, which mimics the *in vivo* environment of hepatic fibrosis. Blebbistatin: A small pharmacological inhibitor with high binding affinity for myosin Ⅱ, which blocks the motor protein in an actin-detached state. Actinomyosin complex: Produced when bipolar myosin filaments interact with polymerized actin filaments to exert tension or produce movement. Lamella: A network of actin fibers which forms the outer edge of cellular protrusions.

Peer review

It's an interesting study and excellent.

REFERENCES

1 **Rockey DC**. Hepatic fibrosis, stellate cells, and portal hypertension. *Clin Liver Dis* 2006; **10**: 459-479, vii-viii
2 **Maher JJ**, McGuire RF. Extracellular matrix gene expression increases preferentially in rat lipocytes and sinusoidal endothelial cells during hepatic fibrosis in vivo. *J Clin Invest* 1990; **86**: 1641-1648
3 **Thimgan MS**, Yee HF. Quantitation of rat hepatic stellate cell contraction: stellate cells' contribution to sinusoidal resistance. *Am J Physiol* 1999; **277**: G137-G143
4 **Wake K**. Perisinusoidal stellate cells (fat-storing cells, interstitial cells, lipocytes), their related structure in and around the liver sinusoids, and vitamin A-storing cells in extrahepatic organs. *Int Rev Cytol* 1980; **66**: 303-353
3 **Thimgan MS**, Yee HF. Quantitation of rat hepatic stellate cell contraction: stellate cells' contribution to sinusoidal resistance. *Am J Physiol* 1999; **277**: G137-G143
4 **Wake K**. Perisinusoidal stellate cells (fat-storing cells, interstitial cells, lipocytes), their related structure in and around the liver sinusoids, and vitamin A-storing cells in extrahepatic organs. *Int Rev Cytol* 1980; **66**: 303-353
5 **Eng FJ**, Friedman SL. Fibrogenesis I. New insights into hepatic stellate cell activation: the simple becomes complex. *Am J Physiol Gastrointest Liver Physiol* 2000; **279**: G7-G11
6 **Bataller R**, Brenner DA. Liver fibrosis. *J Clin Invest* 2005; **115**: 209-218
7 **Friedman SL**. Liver fibrosis -- from bench to bedside. *J Hepatol* 2003; **38 Suppl 1**: S38-S53
8 **Kawada N**, Tran-Thi TA, Klein H, Decker K. The contraction of hepatic stellate (Ito) cells stimulated with vasoactive substances. Possible involvement of endothelin 1 and nitric oxide in the regulation of the sinusoidal tonus. *Eur J Biochem* 1993; **213**: 815-823
9 **Rockey DC**, Housset CN, Friedman SL. Activation-dependent contractility of rat hepatic lipocytes in culture and in vivo. *J Clin Invest* 1993; **92**: 1795-1804
10 **Bauer M**, Paquette NC, Zhang JX, Bauer I, Pannen BH, Kleeberger SR, Clemens MG. Chronic ethanol consumption increases hepatic sinusoidal contractile response to endothelin-1 in the rat. *Hepatology* 1995; **22**: 1565-1576
11 **Zhang JX**, Pegoli W, Clemens MG. Endothelin-1 induces direct constriction of hepatic sinusoids. *Am J Physiol* 1994; **266**: G624-G632
12 **Melton AC**, Yee HF. Hepatic stellate cell protrusions couple platelet-derived growth factor-BB to chemotaxis. *Hepatology* 2007; **45**: 1446-1453
13 **Bresnick AR**. Molecular mechanisms of nonmuscle myosin-II regulation. *Curr Opin Cell Biol* 1999; **11**: 26-33
14 **Golomb E**, Ma X, Jana SS, Preston YA, Kawamoto S, Shoham NG, Goldin E, Conti MA, Sellers JR, Adelstein RS. Identification and characterization of nonmuscle myosin II-C, a new member of the myosin II family. *J Biol Chem* 2004; **279**: 2800-2808
15 **Katsuragawa Y**, Yanagisawa M, Inoue A, Masaki T. Two distinct nonmuscle myosin-heavy-chain mRNAs are differentially expressed in various chicken tissues. Identification of a novel gene family of vertebrate non-sarcomeric myosin heavy chains. *Eur J Biochem* 1989; **184**: 611-616
16 **Simons M**, Wang M, McBride OW, Kawamoto S, Yamakawa K, Gdula D, Adelstein RS, Weir L. Human nonmuscle myosin heavy chains are encoded by two genes located on different chromosomes. *Circ Res* 1991; **69**: 530-539
17 **Kovács M**, Wang F, Hu A, Zhang Y, Sellers JR. Functional divergence of human cytoplasmic myosin II: kinetic characterization of the non-muscle IIA isoform. *J Biol Chem* 2003; **278**: 38132-38140
18 **Liu Z**, van Grunsven LA, Van Rossen E, Schroyen B, Timmermans JP, Geerts A, Reynaert H. Blebbistatin inhibits contraction and accelerates migration in mouse hepatic stellate cells. *Br J Pharmacol* 2010; **159**: 304-315
19 **Lo CM**, Buxton DB, Chua GC, Dembo M, Adelstein RS, Wang YL. Nonmuscle myosin IIb is involved in the guidance of fibroblast migration. *Mol Biol Cell* 2004; **15**: 982-989
20 **Limouze J**, Straight AF, Mitchison T, Sellers JR. Specificity of blebbistatin, an inhibitor of myosin II. *J Muscle Res Cell Motil* 2004; **25**: 337-341
21 **Eddinger TJ**, Meer DP, Miner AS, Meehl J, Rovner AS, Ratz PH. Potent inhibition of arterial smooth muscle tonic contractions by the selective myosin II inhibitor, blebbistatin. *J Pharmacol Exp Ther* 2007; **320**: 865-870
22 **Kovács M**, Tóth J, Hetényi C, Málnási-Csizmadia A, Sellers JR. Mechanism of blebbistatin inhibition of myosin II. *J Biol Chem* 2004; **279**: 35557-35563
23 **Straight AF**, Cheung A, Limouze J, Chen I, Westwood NJ, Sellers JR, Mitchison TJ. Dissecting temporal and spatial control of cytokinesis with a myosin II Inhibitor. *Science* 2003; **299**: 1743-1747
24 **Lakner AM**, Moore CC, Gulledge AA, Schrum LW. Daily genetic profiling indicates JAK/STAT signaling promotes early hepatic stellate cell transdifferentiation. *World J Gastroenterol* 2010; **16**: 5047-5056
25 **Rippe RA**, Almounajed G, Brenner DA. Sp1 binding activity increases in activated Ito cells. *Hepatology* 1995; **22**: 241-251
26 **Obungu VH**, Lee Burns A, Agarwal SK, Chandrasekharapa SC, Adelstein RS, Marx SJ. Menin, a tumor suppressor, associates with nonmuscle myosin II-A heavy chain. *Oncogene* 2003; **22**: 6347-6358
27 **Karaa A**, Thompson KJ, McKillop IH, Clemens MG, Schrum LW. S-adenosyl-L-methionine attenuates oxidative stress and hepatic stellate cell activation in an ethanol-LPS-induced fibrotic rat model. *Shock* 2008; **30**: 197-205
28 **Tsukamoto H**, Matsuoka M, French SW. Experimental models of hepatic fibrosis: a review. *Semin Liver Dis* 1990; **10**: 56-65

29 **Rockey DC**, Boyles JK, Gabbiani G, Friedman SL. Rat hepatic lipocytes express smooth muscle actin upon activation in vivo and in culture. *J Submicrosc Cytol Pathol* 1992; **24**: 193-203

30 **Kawada N**, Kuroki T, Kobayashi K, Inoue M, Kaneda K, Decker K. Action of endothelins on hepatic stellate cells. *J Gastroenterol* 1995; **30**: 731-738

31 **Liu Z**, Rossen EV, Timmermans JP, Geerts A, van Grunsven LA, Reynaert H. Distinct roles for non-muscle myosin II isoforms in mouse hepatic stellate cells. *J Hepatol* 2011; **54**: 132-141

32 **Vicente-Manzanares M**, Ma X, Adelstein RS, Horwitz AR. Non-muscle myosin II takes centre stage in cell adhesion and migration. *Nat Rev Mol Cell Biol* 2009; **10**: 778-790

33 **Kolega J**. Cytoplasmic dynamics of myosin IIA and IIB: spatial 'sorting' of isoforms in locomoting cells. *J Cell Sci* 1998; **111 (Pt 15)**: 2085-2095

34 **Vicente-Manzanares M**, Zareno J, Whitmore L, Choi CK, Horwitz AF. Regulation of protrusion, adhesion dynamics, and polarity by myosins IIA and IIB in migrating cells. *J Cell Biol* 2007; **176**: 573-580

35 **Meshel AS**, Wei Q, Adelstein RS, Sheetz MP. Basic mechanism of three-dimensional collagen fibre transport by fibroblasts. *Nat Cell Biol* 2005; **7**: 157-164

36 **Kountouras J**, Billing BH, Scheuer PJ. Prolonged bile duct obstruction: a new experimental model for cirrhosis in the rat. *Br J Exp Pathol* 1984; **65**: 305-311

37 **Wirz W**, Antoine M, Tag CG, Gressner AM, Korff T, Hellerbrand C, Kiefer P. Hepatic stellate cells display a functional vascular smooth muscle cell phenotype in a three-dimensional co-culture model with endothelial cells. *Differentiation* 2008; **76**: 784-794

38 **Dudek SM**, Garcia JG. Rho family of guanine exchange factors (GEFs) in cellular activation: who's dancing? And with whom? *Circ Res* 2003; **93**: 794-795

39 **Katoh K**, Kano Y, Amano M, Onishi H, Kaibuchi K, Fujiwara K. Rho-kinase--mediated contraction of isolated stress fibers. *J Cell Biol* 2001; **153**: 569-584

40 **Kawada N**, Seki S, Kuroki T, Kaneda K. ROCK inhibitor Y-27632 attenuates stellate cell contraction and portal pressure increase induced by endothelin-1. *Biochem Biophys Res Commun* 1999; **266**: 296-300

41 **Kelley CA**, Adelstein RS. The 204-kDa smooth muscle myosin heavy chain is phosphorylated in intact cells by casein kinase II on a serine near the carboxyl terminus. *J Biol Chem* 1990; **265**: 17876-17882

42 **van Leeuwen FN**, van Delft S, Kain HE, van der Kammen RA, Collard JG. Rac regulates phosphorylation of the myosin-II heavy chain, actinomyosin disassembly and cell spreading. *Nat Cell Biol* 1999; **1**: 242-248

43 **Wilson JR**, Biden TJ, Ludowyke RI. Increases in phosphorylation of the myosin II heavy chain, but not regulatory light chains, correlate with insulin secretion in rat pancreatic islets and RINm5F cells. *Diabetes* 1999; **48**: 2383-2389

44 **Moussavi RS**, Kelley CA, Adelstein RS. Phosphorylation of vertebrate nonmuscle and smooth muscle myosin heavy chains and light chains. *Mol Cell Biochem* 1993; **127-128**: 219-227

45 **Ramamurthy B**, Yengo CM, Straight AF, Mitchison TJ, Sweeney HL. Kinetic mechanism of blebbistatin inhibition of nonmuscle myosin IIb. *Biochemistry* 2004; **43**: 14832-14839

46 **Hotchkiss RS**, Karl IE. The pathophysiology and treatment of sepsis. *N Engl J Med* 2003; **348**: 138-150

47 **Khanna A**, Rossman JE, Fung HL, Caty MG. Intestinal and hemodynamic impairment following mesenteric ischemia/reperfusion. *J Surg Res* 2001; **99**: 114-119

48 **Keller SA**, Paxian M, Lee SM, Clemens MG, Huynh T. Kupffer cell ablation attenuates cyclooxygenase-2 expression after trauma and sepsis. *J Surg Res* 2005; **124**: 126-133

49 **Huynh T**, Nguyen N, Keller S, Moore C, Shin MC, McKillop IH. Reducing leukocyte trafficking preserves hepatic function after sepsis. *J Trauma* 2010; **69**: 360-367

50 **Keller SA**, Paxian M, Ashburn JH, Clemens MG, Huynh T. Kupffer cell ablation improves hepatic microcirculation after trauma and sepsis. *J Trauma* 2005; **58**: 740-749; discussion 749-751

51 **Cardenas A**, Gines P. Portal hypertension. *Curr Opin Gastroenterol* 2009; **25**: 195-201

52 **Rockey DC**. Noninvasive assessment of liver fibrosis and portal hypertension with transient elastography. *Gastroenterology* 2008; **134**: 8-14

53 **Hernández-Guerra M**, García-Pagán JC, Bosch J. Increased hepatic resistance: a new target in the pharmacologic therapy of portal hypertension. *J Clin Gastroenterol* 2005; **39**: S131-S137

54 **Jakob SM**. Splanchnic blood flow in low-flow states. *Anesth Analg* 2003; **96**: 1129-138, table of contents

S- Editor Zhang HN **L- Editor** Roemmele A **E- Editor** Zhang L